THE AMERICAN SOCIETY OF MECHANICAL ENGINEERS
345 E. 47th St., New York, N.Y. 10017

95-GT-357

The Application of Thin Film Gauges on Flexible Plastic Substrates to the Gas Turbine Situation

S. M. Guo, M. C. Spencer, G. D. Lock and T. V. Jones
Department of Engineering Science,
University of Oxford,
United Kingdom

N. W. Harvey
Rolls-Royce plc.,
Derby,
United Kingdom

Abstract

Thin film heat transfer gauges have been instrumented onto flexible plastic substrates which can be adhesively bonded to plastic or metal models. These new gauges employ standard analysis techniques to yield the heat flux to the model surface and have significant advantages over gauges fired onto machinable glass or those used with metal models coated with enamel. The main advantage is that the construction of the gauges is predictable and uniform, and thus calibration for thickness and geometric properties is not required.

The new gauges have been used to measure the heat transfer to an annular turbine nozzle guide vane in the Oxford University Cold Heat Transfer Tunnel. Engine-representative Mach and Reynolds numbers were employed and the free-stream turbulence intensity at NGV inlet was 13%.

The vanes were either precooled or preheated to create a range of different thermal boundary conditions. The gauges were mounted on both perspex and aluminium NGVs and the heat transfer coefficient was obtained from the surface temperature history using either a single layer analysis (for perspex) or double layer (for aluminium) analysis. The surface temperature and heat transfer levels were also measured using rough and polished liquid crystals under similar conditions. The measurements have been compared with computational predictions.

Nomenclature

a	Depth of insulating layer
b	Finite depth of model
c	Specific heat
c_f	Skin friction coefficient
h	Heat transfer coefficient
k	Thermal conductivity
$\dot{q}$	Heat flux
r	Recovery factor
R	Restistance
s	Laplace Transform variable
t	Time
T	Temperature
u	Velocity
x	Distance into the substrate
y^+	Roughness Reynolds number
α	Temperature coefficient of resistance
β	Thermal diffusivity
ν	Viscosity
ρ	Density
τ	Data time interval

1 Introduction

Changes in the resistance of thin film metal layers can be related to their temperature. When placed on a substrate of known thermal properties, measurements

Presented at the International Gas Turbine and Aeroengine Congress and Exposition
Houston, Texas - June 5-8, 1995

of the temperature history of such metal films, coupled with the appropriate analytical model, can lead to the calculation of the surface heat flux history (Schultz and Jones 1973, Doorly and Oldfield 1987).

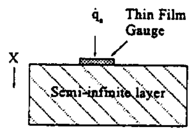

Figure 1a : Semi-infinite gauge

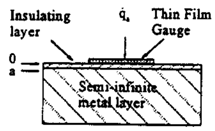

Figure 1b : Layered gauge with semi-infinite metal substrate

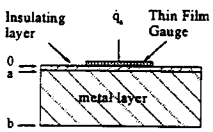

Figure 1c : Layered gauge with finite-depth metal substrate

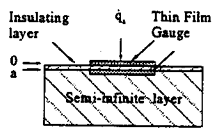

Figure 1d : Two-layered gauge

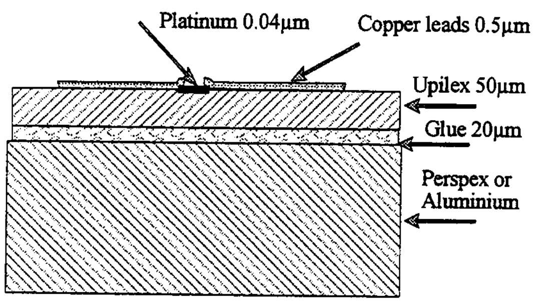

Figure 2 : Schematic diagram of thin film gauge

The use of such gauges for measuring heat transfer rates to turbine blades in short-duration transient cascade facilities is well documented (Schultz and Jones 1973, Oldfield et al 1978, Jones et al 1993). As well as measuring the surface heat transfer rates, the interpretation of these signals can yield much useful information about the gas flow and boundary layers.

Three general types of surface thin film gauges have been reported. The first type are mounted on a substrate which is considered semi-infinite, as shown in figure 1a. A typical example of this type would be a thin film nickel or platinum resistance thermometer fired onto a macor, quartz or glass substrate (Shultz and Jones 1973, Oldfield et al 1978, Oldfield et al 1981). The use of machinable glass is expensive and, for structural reasons, limited to stationary cascade facilities.

Thin film gauges can be utilised on metal turbine blades. This second type are layered gauges where a thin insulating layer such as vitreous enamel is sprayed over the model (usually made of metal) which has different thermal properties (Doorly and Oldfield 1986, Ainsworth et al 1989). For the purposes of data analysis, these layered gauges may be considered to have a semi-infinite metal substrate (figure 1b) or a finite-depth metal substrate (figure 1c) and techniques to analyse the gauge response have been reported (Doorly and Oldfield 1987). Coating a metal blade with enamel requires careful matching of metal with enamel and involves heating the assembly. Furthermore, the accuracy of the data obtained with these layered gauges depends upon a knowledge of the thickness of the enamel layer which can vary around the model surface.

Epstein et al (1985) have made extensive use of thin film gauges at MIT. In addition to using single-layer gauges, they have developed two-layered gauges where the temperature difference across a thermal resistance of accurately known properties and dimensions is measured (figure 1d). The thermal resistance layer (e.g. kapton) is adhesively bonded to the model. The accuracy of the measurements from two-layered gauges depends upon the temperature difference across the insulating layer and they have limited use in situations where the difference in temperature between the model and gas is small. Kapton-mounted gauges have previously been used (Epstein et al 1985) on metal blades. These employed serpentine nickel films on either side of the plastic. Holes penetrated the plastic to give electrical access to the lower film. In another reported study (Cook et al 1991) a kapton layer was achieved by immersing a blade in a liquid solution which dried to give the desired layer. The thin films were subsequently sputtered on the assembly.

This paper describes the use of a new type of thin film heat transfer gauge which has been developed at the Osney Laboratory at Oxford (Jones 1988) by Jones and others. The thin film gauges have been instrumented onto flexible, upilex plastic sheets (50 μm thick) which are easily adhesively bonded to perspex or metal models. These gauges avoid the difficulties involved with enamel coatings, have an insulating layer of uniform thickness and known thermal properties and dimensions, and can accommodate models with highly curved surfaces. The well known semi-infinite or layered gauge analysis techniques can be employed to yield the heat flux in the normal manner. The application of these gauges to the gas turbine situation is demonstrated and the measurements are compared with heat transfer levels obtained using the transient liquid crystal technique.

2 Thin Film Gauges

The Osney Laboratory at Oxford has developed a facility which specialises in manufacturing large arrays of thin films. In the past, thin film gauges have been employed extensively where the platinum films were deposited on pyrex, machineable glass or enamel and in some cases using kapton substrates, either as thin sheets or using dipped models. All of the above methods were time consuming and required complex manufacture. More importantly, very careful calibration using pulsed techniques were required at each gauge position. The great advantage of the new gauges is that the construction is predictable and uniform. Thus the gauges do not need calibration for their thickness and geometric properties, only for their temperature coefficient of resistance. The latter calibration is easily performed. Furthermore, the gauges used in the present experiments are manufactured relatively simply and thus models may be instrumented simply and relatively inexpensively, bringing the application of thin film instrumentation to a routine procedure.

A detailed description of the manufacturing process is available in laboratory reports (Hofeldt 1993, Guo 1994). A brief description is presented here.

The thin film gauges are fabricated from 0.04 μm thick pure platinum. The platinum is sputtered onto thin (50 μm) sheets of upilex using an R-F magnetron. The sheet is then covered in a thin (0.5 μm) layer of copper using sputtering (in 0.005 mbar of Argon) and evaporation (in 10^{-5} mbar of Argon) techniques. Under darkened conditions, aerosol photoresist is sprayed over the surface. This surface is later exposed to UV light under a mask which leaves a pattern with the desired geometry of the leads after developing and etching. A schematic of a typical gauge and upilex layer is shown in figure 2. The gauges can be manufactured in various sizes and patterns. The dimensions of the gauges used in the experiments described here were 0.1 by 2.0 mm. Typically the gauge and lead resistances are 50 and 1 Ω respectively.

When the upilex sheet is mounted on perspex, the thin film gauges can be considered to be on a semi-infinite substrate (figure 1a) because the thermal properties of upilex, glue and perspex are similar. This was tested in a controlled calibration experiment using gauges mounted on a flat plate and comparing the surface temperature histories with those recorded simultaneously with a fast-response thermocouple mounted directly onto the perspex surface. When the upilex sheet is mounted on a substrate with different thermal properties (e.g., metal), the system has to be analysed as a layered gauge (figure 1b or 1c). Calibration tests were used to establish the thickness of the upilex/glue insulating layer (dimension a in figure 1b and 1c) which had a uniform value around the model. This was done by comparing the heat flux signals from the layered gauges with those simultaneously measured from the fast-response thermocouple mounted on perspex.

For the application of these gauges to measure heat transfer to gas turbine blades, the flexible sheet of upilex was wrapped around and glued to either perspex or aluminium nozzle guide vanes (NGVs). There is no difficulty in making the glue layer a uniform thickness. The thickness of the glue is $< 20\mu$m and so most of the gauge thickness is the upilex ($\sim 50\mu$m). This glue is a premanufactured adhesive layer of predictable, uniform thickness.

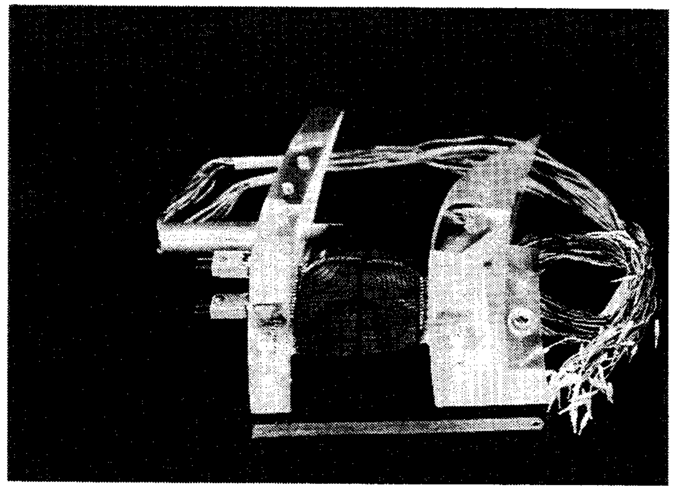

Figure 3a : Thin film gauges on the suction surface

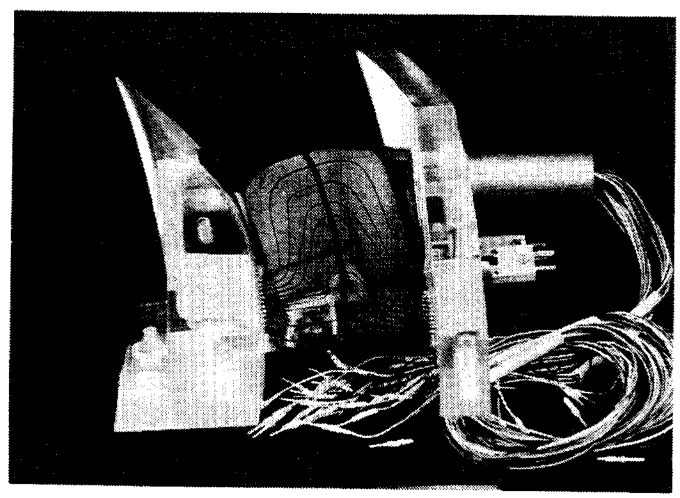

Figure 3b : Thin film gauges on the pressure surface

A typical set of thin films on a perspex NGV is shown in figure 3a and 3b. There are 11 gauges on the pressure surface and 15 gauges on the suction surface, all aligned on a streamline along midspan. Gauges were also been mounted at 10 and 90% span. In order to accommodate the curvature of the NGV surface, the plastic insulating sheets were cut into several pieces and glued separately onto the model. The gaps between sheets were far from the gauges and filled with a suitable filler to leave an extremely smooth surface.

The thin film gauges described in this paper were operated in a constant current mode. In this mode of operation, a small, constant sensing current is passed through the thin film in order to generate a change in voltage proportional to the change of film resistance and temperature. The surface temperature (T) is related to the gauge resistance using $R = R_0(1+\alpha(T-20))$, where R_0 is the resistance at 20 C and α is the temperature coefficient of resistance. The value of α was obtained from calibration in a hot water bath and was typically $\sim 0.001\ \mathrm{K}^{-1}$. A great advantage of the gauges was the uniformity of the construction. This meant that the thermal properties were the same for all gauges and positions, and once this had been determined by calibration on the flat plate referred to above then α was the only parameter requiring calibration.

The new thin film gauges have a wide range of applications. They are presently being used in a rotor experiment (Prosser, 1994), they can be used as hot films (Bown et al 1994) and for transition studies (Bown et al 1994, Hofeldt 1993). The gauges may also be used for film cooled models. The upilex sheets are wrapped around the model as described above and subsequently holes may be drilled in the layer to produce film cooling geometries. Careful drilling is necessary and the film cooling holes should be drilled in the underlying model before mounting the plastic. The use of numerically-controlled machines to ensure accuracy in the process is beneficial. The analysis of the signals from the film cooled situation is identical to that described for the unfilm-cooled gauges, independent of thermal boundary conditions.

3 Data Reduction

The voltage history from the gauges leads to measurements of the change in the gauge resistance with time. From the temperature-resistance calibration a measurement of the surface temperature history is obtained. For the perspex blade, the substrate of the upilex, glue and perspex was considered to be a single, homogeneous material. The thin films on the upilex sheet with the metal blade was considered to be a layered gauge, with the upilex and glue a homogeneous material.

Perspex NGV

For the perspex NGV, the model insulating substrate (figure 1a) is considered semi-infinite and the one-dimensional heat conduction equation

$$\frac{\partial^2 T}{\partial x^2} = \frac{1}{\beta}\frac{\partial T}{\partial t} \quad (1)$$

may be solved for the heat transfer rate $\dot{q}$ at the surface. The boundary conditions for $\dot{q}(x,t)$ and $T(x,t)$ are $\dot{q}(0,t) = -k\partial T/\partial x$, $T(\infty,t) = T_0$, and $T(x,0) = T_0$. In the above equations T is the temperature, T_0 is the initial temperature, t the time, x the dimension normal to the surface, and β and k are the thermal diffusivity and thermal conductivity of the substrate. The time variation of $\dot{q}$ is evaluated from the surface temperature history using the Laplace transform method described in Oldfield et al (1978), viz.,

$$\dot{q}(m\tau) = 2\sqrt{\frac{\rho c k}{\pi\tau}}\sum_{n=0}^{m}(T_{n+1}+T_{n-1}-2T_n)(m-n)^{0.5}, \quad (2)$$

where τ is the time interval between data points.

Metal NGV

For the metal blade a layered model must be used to calculate the heat transfer rate from the surface temperature history. Two different methods were used. The first assumes that the metal blade appears infinitely thick to the thermal waves propagating from the surface, i.e., the aluminium is semi-infinite. This method is accurate over most of the NGV surface but not in the trailing edge region where the thickness of the blade is as thin as 1 mm. A second method, using a numerical technique, has been used to account for the finite thickness of the metal in this region.

For the case of a semi-infinite backwall (figure 1b) there is a thermally insulating layer ($i = 1, 0 < x < a$) and the metal substrate ($i = 2, a < x < \infty$), where a is the thickness of the upilex and glue. The governing equation is

$$\frac{\partial^2 T_i}{\partial x^2} = \frac{1}{\beta_i}\frac{\partial T_i}{\partial t},\ i = 1,2 \quad (3)$$

with the boundary conditions $\dot{q} = -k\partial T_1/\partial x$ at $x = 0$, $T_1 = T_2$ at $x = a$, $-k_1\partial T_1/\partial x = -k_2\partial T_2/\partial x$ at $x = a$ and $\partial T_2/\partial x = 0$ at $x = \infty$. A solution to these equations, using Laplace Transforms, is presented in references (Schultz and Jones 1973, Doorly and Oldfield 1987). Solving for $\overline{T_1}$ and $\overline{T_2}$ yields,

$$\overline{T_1} = \frac{\dot{q_s}}{k_1\Lambda_1}\left(\frac{(1+\sigma)e^{(-(x-a)\Lambda_1)} + (1-\sigma)e^{((x-a)\Lambda_1)}}{(1+\sigma)e^{(a\Lambda_1)} - (1-\sigma)e^{(-a\Lambda_1)}}\right) \quad (4)$$

$$\overline{T_2} = \frac{2\dot{q_s}}{k_1\Lambda_1}\left(\frac{e^{((x-a)\Lambda_2)}}{(1+\sigma)e^{(a\Lambda_1)} - (1-\sigma)e^{(-a\Lambda_1)}}\right) \quad (5)$$

where $\Lambda_i = \sqrt{s/\beta_i}$, $\sigma = \sqrt{(\rho_2 c_2 k_2)/(\rho_1 c_1 k_1)}$, $\dot{q_s}$ is the heat flux at $x = 0$, ρ and c are the substrate density and specific heat capacity, and s is the Laplace transform variable.

For the case of a finite depth metal substrate (figure 1c), the model has a thermally insulating layer ($i = 1, 0 < x < a$) of upilex and glue, and a metal substrate ($i = 2, a < x < b$) of finite dimension $b - a$. For this case, equation (3) is solved with the same boundary conditions as immediately above except that $\partial T_2/\partial x = 0$ at $x = b$, not at $x = \infty$. A solution for this case has been obtained (Doorly and Oldfield 1987) but a finite difference technique (Whitaker 1977) was preferred here. This numerical technique is described in detail by Guo (1994). It should be noted that the finite depth analysis method was only required near the trailing edge of the blade and that calculations using this method were in agreement with the semi-infinite backwall method in all other regions.

4 Gas Turbine Application

Heat transfer measurements using thin film gauges mounted on flexible plastic substrates have been performed in the Oxford University Cold Heat Transfer Tunnel (Martinez-Botas et al 1993, 1994), or CHTT. This tunnel is described in detail in these two references and was originally a linear cascade (Baines et al 1982). The test section of the tunnel is an annular cascade of 36 NGVs at 1.4 times larger than engine scale. The test duration of the facility (about 7 seconds at engine design conditions) enables transient techniques to be employed. The tunnel allows an independent variation of Reynolds and Mach numbers, or equivalently the upstream and downstream pressures can be independently and continuously varied. Details of the NGV geometry are given in table 1.

Table 1: **NGV Details**

Mid-span axial chord	0.0664 m
Mean pitch at exit	0.09718 m
Span at exit	0.08076 m
Turning angle	73°
Throat area	0.08056 m^2
Mean blade diameter	1.113 m

A schematic diagram of the CHTT is shown in figure 4. The operation of the tunnel is controlled by pneumatically-activated ball valves. Air flows from the high pressure reservoir (31 m^3 at 3 MPa) into a regulator system from which part of the flow enters an ejector. The remainder passes into the annular test section containing the NGVs, subsequently exhausting to atmosphere.

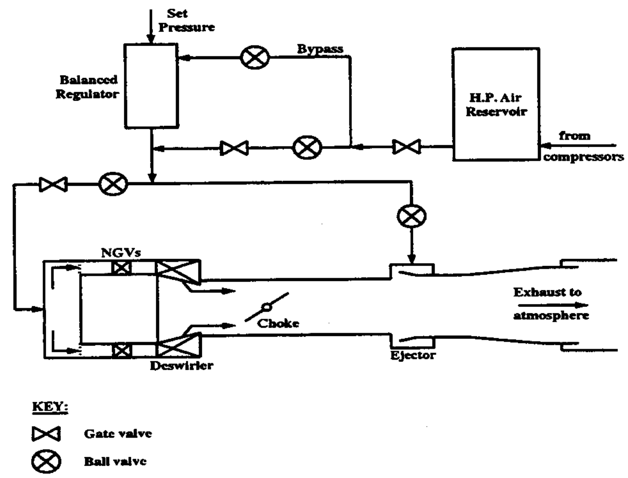

Figure 4 : Schematic of the CHTT

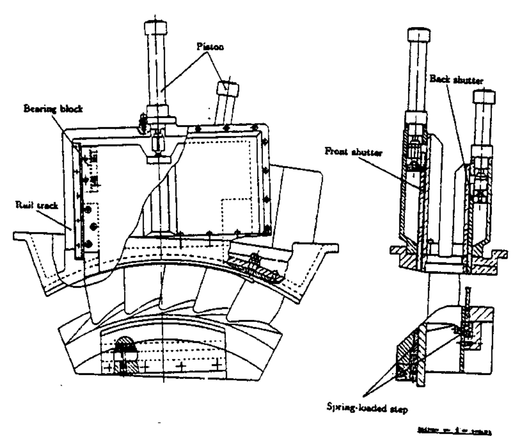

Figure 5 : Heat Transfer Cassette

For the experiments reported here, five NGV aerofoil surfaces and end walls were preheated or precooled before running the tunnel by isolating four passages of the annulus with a shutter mechanism and cassette as illustrated in figure 5. The central NGV in the cassette was instrumented either with the thin film gauges or coated with narrow-band liquid crystals. A detailed description of the application of the transient liquid crystal technique to the CHTT is provided by Martinez-Botas et al (1994) and only the instrumentation for thin film gauge measurements will be discussed here.

The instrumentation required to operate the thin film gauges is standard and discussed in detail in Shultz and Jones (1973) and in Oldfield et al (1978). A constant current source was used to power the thin film gauges. The current was minimised (< 1 mA) to avoid significant heating of the thin films. The voltage history of these gauges were amplified and then recorded at 2 kHz using an analogue to digital converter and a 386 pc. Higher frequency information can be obtained (on fewer channels) up to a rate of 300 kHz. Surface temperature histories were also recorded using two thermocouples on the NGV surface and a third thermocouple is used to measure the free-stream air temperature.

5 Results and Discussion

All of the results presented here are at engine design conditions (Re $= 1.95 \times 10^6$ and $M_{exit} = 0.96$) and with a free-stream turbulence intensity and length scale of 13% and 21 mm at NGV inlet. A typical surface temperature history from a gauge on the pressure surface of a preheated ($T_0 \sim 60$ C) perspex NGV is shown in figure 6a. The CHTT begins operation at 3 s and, with the shutters lowered, a small amount of cold air leaks into the cassette until the shutters open (opening time 60 ms) at 4.6 s. The surface temperature is seen to drop until the tunnel is shut off at 7 s and then rises as the surface is reheated from the substrate. The heat transfer rate, calculated from equation (2), is shown as a function of time in figure 6b.

Figure 6c is a plot of the heat transfer coefficient (h) as a function of time. This is calculated from

$$h = \frac{\dot{q}}{T_s - T_g} \tag{6}$$

where T_s is the surface temperature and T_g is the local gas recovery temperature (Jones 1991) defined by $T_g = T_\infty(1 + r(\gamma - 1)M_\infty^2/2)$ with T_∞ and M_∞ being the local gas temperature and Mach number, and $r = 0.87$ is the recovery factor. The total temperature history at inlet to the CHTT is shown in figure 6d and the local recovery temperature is calculated using the Mach number distribution around the NGV (Martinez-Botas et al 1994). Note that h is at a constant level during the 2.5 s that the gauge encounters the steady flow.

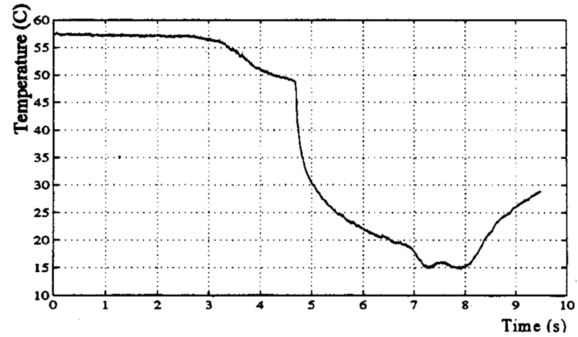

Figure 6a : Surface Temperature History

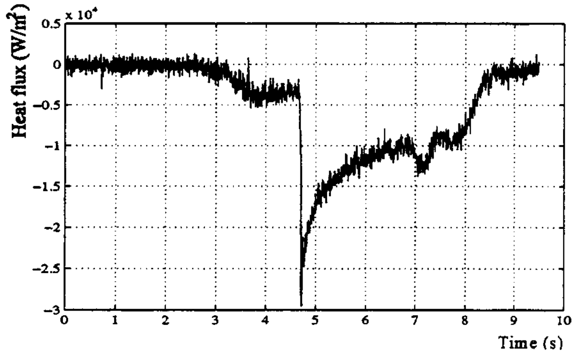

Figure 6b : Surface Heat Flux History

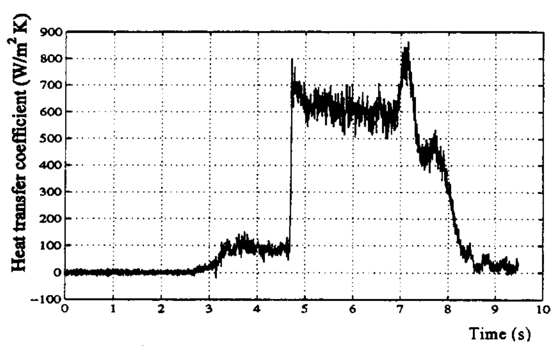

Figure 6c : Heat Transfer History

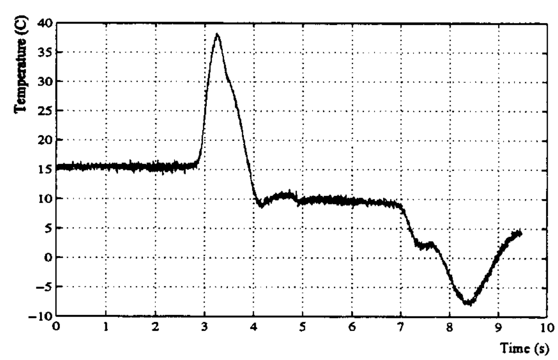

Figure 6d : Gas temperature history

The heat transfer coefficient measured by all gauges, each averaged over the steady portion of the run, is plotted against fraction of surface distance along the 10, 50 and 90% span streamlines in figure 7. This figure shows that along the midspan, h falls from a stagnation level of 650 W/m^2K to a minimum of 350 W/m^2K at about 25% surface distance on the pressure surface. The heat transfer coefficient then rises to approximately 800 W/m^2K at the trailing edge. On the suction surface, transition is seen to occur at about 45% surface distance. The turbulent level of h is about 650 W/m^2K. Uncertainty levels in the measurement of the heat transfer coefficient are estimated to be $\pm 5\%$.

The heat transfer levels on the pressure surface do not vary greatly with different span positions. On the suction surface the highest levels of heat transfer occur at 90% span. At about 60% surface distance the heat transfer level along the 90% spanline drops significantly and dips below the midspan level at the trailing edge. This decrease in heat transfer level occurs in a region influenced by secondary flows. This region of separated flow on the suction surface has been identified using flow visualisation with coloured oil as shown in figure 8. The reduction in the heat transfer level is not as obvious at 10% span where, due to the radial pressure gradient, the separation lines do not extend as far from the hub end wall.

Figure 8 : Flow visualization on the suction surface 100% span (casing) at top

Another plot of heat transfer coefficient (W/m^2K) versus fraction of surface distance along the midspan streamline is shown in figure 9. This data was acquired over a range of thermal boundary conditions and different directions of heat flux. Various symbols appear in this figure and represent data taken from preheated ($T_0 \sim 60$ C), precooled ($T_0 \sim -15$ C), or near ambient ($T_0 \sim 20$ C) conditions, and from either perspex or aluminium NGVs. The local gas recovery temperature used in the calculation of the heat transfer coefficient varied between 5 and 18 C around the NGV midspan. The data indicates that the measurements using the aluminium and perspex materials yield the same heat transfer coefficient when the appropriate analysis technique is employed. The measurements also show that the thermal boundary conditions have little, if any, influence on the distribution of heat transfer coefficient.

6 Comparison with Liquid Crystals

Figures 10 to 12 compare the thin film gauge heat transfer results with those made using the transient liquid crystal technique (Martinez-Botas et al 1994). The data from the liquid crystals exhibit similar features to those obtained using the thin film gauges, including the reduction in heat transfer coefficient in the regions influenced by secondary flow. The differences in the heat transfer levels obtained from the two methods are due to surface roughness.

Different scales of roughness can be obtained by polishing the liquid crystals on the model surface. Unpolished crystals have a roughness (k) of $\sim$ 25 μm and a second set of experiments were performed with semi-polished crystals with a roughness of $\sim$ 10 μm. These figures show that the roughness increases the heat transfer to the pressure surface and alters the transition point on the suction surface despite the large levels of free-stream turbulence. These observations are similar to those found by Turner et al (1985). It should be noted that liquid crystals can be polished down to a very smooth surface for studies of transition phenomena (Bown et al 1994) but this was not pursued in the work presented here.

The value of y^+ (or roughness Reynolds number) (Kays and Crawford 1993),

$$\mathrm{Re}_k = y^+ = \frac{ku_\tau}{\nu} = \frac{ku_\infty\sqrt{c_f/2}}{\nu}$$

has been calculated for different positions along the pressure and suction surfaces and is shown in figure 13. In the above equation k is the roughness dimension, c_f is the skin friction coefficient, u_τ and u_∞ are the local shear velocity and free-stream velocity at NGV exit, and ν is the viscosity. These calculations are an approximation based on a flat plate turbulent boundary layer and have been made in order to estimate whether the roughness of the unpolished and semi-polished liquid crystals on the NGV is likely to effect the heat transfer levels. A value of $\mathrm{Re}_k < 5$ is considered to be hydraulically smooth and a value of $\mathrm{Re}_k > 70$ is considered to be fully rough (Kays and Crawford 1993). In between the

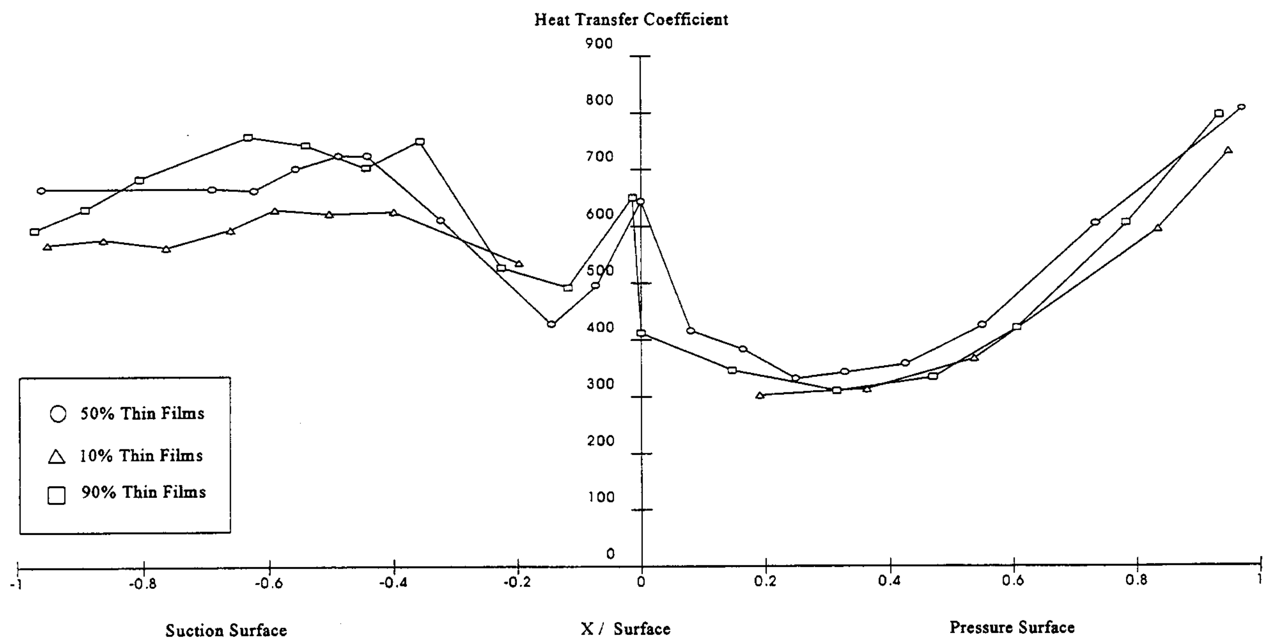

Figure 7 : Heat transfer (W/m^2 K) from the thin film gauges on perspex

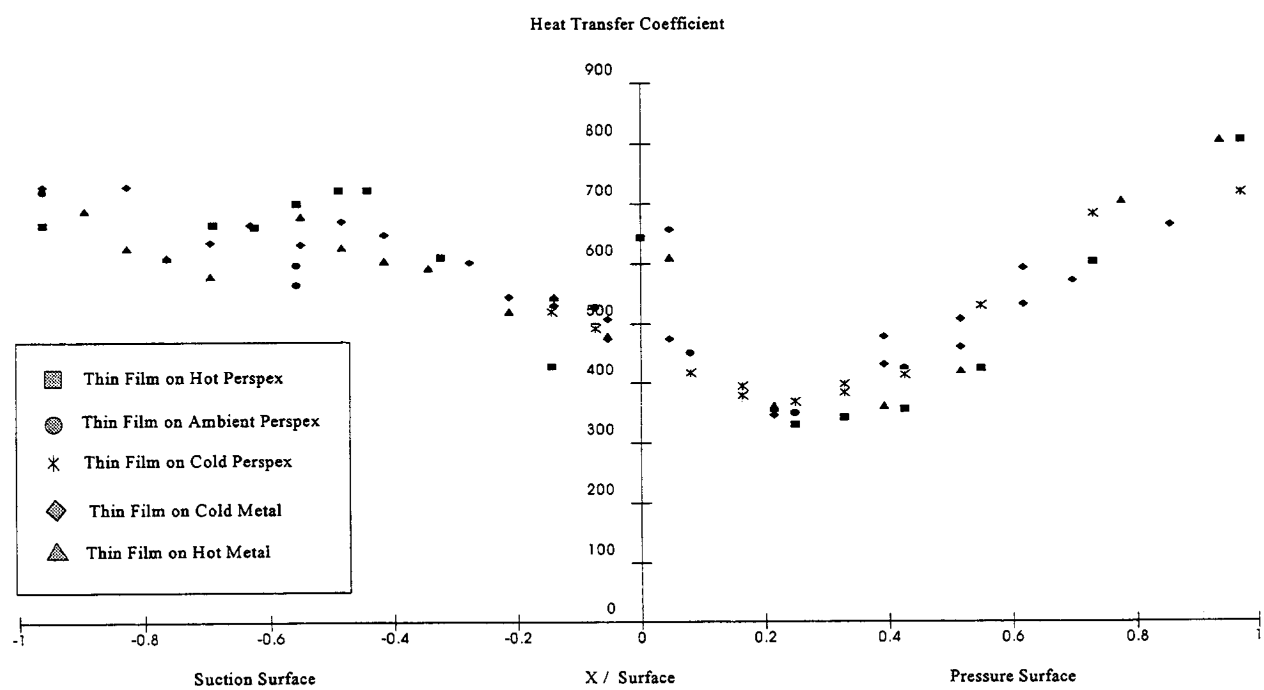

Figure 9 : Heat transfer (W/m^2 K) at midspan with different NGV materials and thermal boundary conditions

surface is considered to be transitionally rough. Figure 13 indicates that the semi-polished surface is transitionally rough at every point and this roughness is likely to effect both the heat transfer levels and the location of the transition point.

A two-dimensional boundary layer heat transfer prediction (Forest 1977) was performed along the NGV midspan at the tunnel conditions and is shown in figure 14, along with the experimental data. The heat transfer coefficients shown are for four different surface roughness levels: 0, 10, 25 and 100 μm. The predictions indicate similar trends to the measured data, including an increase in the heat transfer levels with surface roughness and changes in the location of the transition point on the suction surface despite the high level of free-stream turbulence.

Conclusions

Thin film heat transfer gauges have been instrumented onto flexible, upilex plastic sheets (50 μm thick) which are easily adhesively bonded to perspex or metal models. These gauges avoid the calibration difficulties associated with other methods employing films on insulating coatings as they have an insulating layer of uniform thickness and known thermal properties and dimensions. Also with suitable "cutting" they can accommodate models with multiple curvature. The gauges used in the present experiments are manufactured relatively simply and thus models may be instrumented simply and relatively inexpensively, bringing the application of thin film instrumentation to a routine procedure. The well known semi-infinite or layered gauge analysis techniques can be employed to yield the heat flux in the normal manner.

These new thin film gauges have been used successfully to measure the heat transfer in an annular cascade of NGVs at engine-representative Reynolds and Mach numbers and high levels of free stream turbulence. Both perspex and metal turbine blades were used to make measurements over a range of thermal boundary conditions. The measurements were compared with results obtained using liquid crystals and with numerical predictions. The experiments have shown that for the case of high turbulence flow, thermal boundary layers are of little significance whereas surface roughness plays an important role.

Acknowledgements

This work was funded by Rolls Royce plc. The authors wish to thank Rolls Royce for their support, advice and assistance for this project and for permission to publish the paper. The authors are grateful for the assistance of T. Godfrey and Drs M. Oldfield, R. Martinez-Botas, Z. Wang and P. Ireland.

References

Ainsworth, R. W., Allen, J. L., Davies, M. R. D., Doorly, J. E., Forth, C. J. P., Hilditch, M. A., Oldfield, M. L. G. and Sheard, A. G., 1989, *Developments in Instrumentation and Processing for Transient Heat Transfer Measurements in a Full Stage Model Turbine, ASME J. of Turbomachinery,* **(111)**, pp 20–27.

Baines, N. C., Oldfield, M. L. G., Jones, T. V., Shultz, D. L., King, P. I., and Daniels, L. C., 1982, *A Short-Duration Blowdown Tunnel for Aerodynamic Studies on Gas Turbine Blading,* ASME paper No. 82–GT–312.

Bown, N. W., Cain, T. M., Jones, T. V., Shipley, P. P., and Barry, B., 1994, *In Flight Heat Transfer Measurements on an Aero-Engine Nacelle,* ASME 94-GT-244.

Cook, S. C. P., Kunikyo, T. and Shinohara, J., 1991, *The Direct Deposition of Multiple Hot Film Sensors on a Turbine NGV Using Thin Film Processing Techniques,* ISABE 91-7018.

Doorly, J. E. and Oldfield, M. L G., 1987, *The Theory of Advanced Multi-Layer Thin Film Heat Transfer Gauges,* Int. J. Heat Mass Transfer, **(30)**, 6, 1159-1168.

Doorly, J. E. and Oldfield, M. L G., 1986, *New Heat Transfer Gauges for use on Multi-layered Substrates,* ASME J. Turbomachinery, **(108)**, 1.

Epstein, A. H., Guenette, G. R., Norton, R. J. G., and Cao- Yuzhang, 1985, *High Frequency Response Heat Flux Gauges for Metal Blading,* AGARD-CP-390, Norway.

Forest, A. E., Engineering Predictions of Transitional Boundary Layers, AGARD-CP-224, 1977.

Guo, S. M., 1994, *Thin Film Instrumentation on Plastic Substrates and Applications to Aerodynamics,* First Year Report, Oxford University.

Hofeldt, A., 1993, *Thin Film Techniques and Turbulent Spot Studies,* First Year Report, Oxford University.

Jones, T. V., Oldfield, M. L. G., Ainsworth, R. W. and Arts, T., 1993, *Transient-Cascade Testing,* Chapter 5 of Advanced Methods for Cascade Testing, AGARDOGRAPH 328, AGARD.

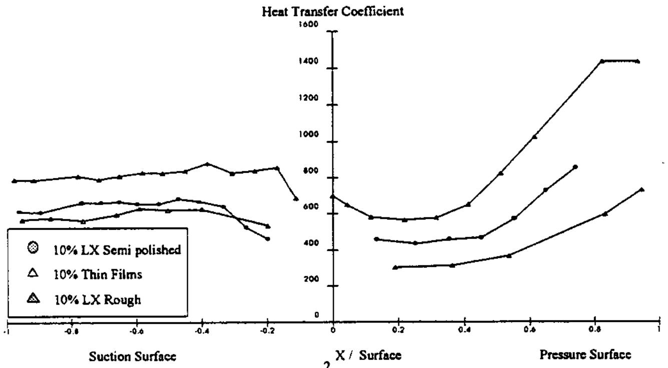

Figure 10 : Heat transfer (W/m^{2}K) from both thin film gauges and liquid crystal (LX) at 10% span

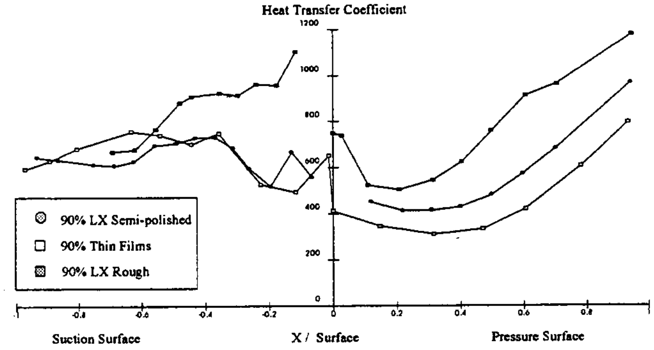

Figure 12 : Heat transfer (W/m^{2}K) from both thin film gauges and liquid crystal (LX) at 90% span

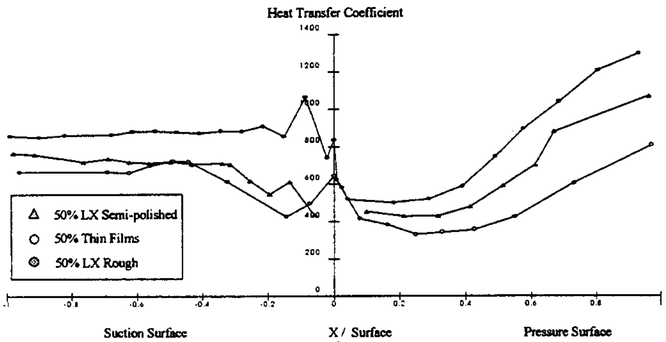

Figure 11 : Heat transfer (W/m^{2}K) from both thin film gauges and liquid crystal (LX) at 50% span

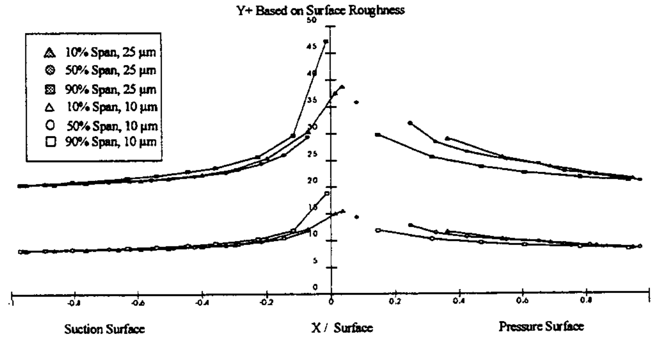

Figure 13 : Roughness parameter along the NGV surface

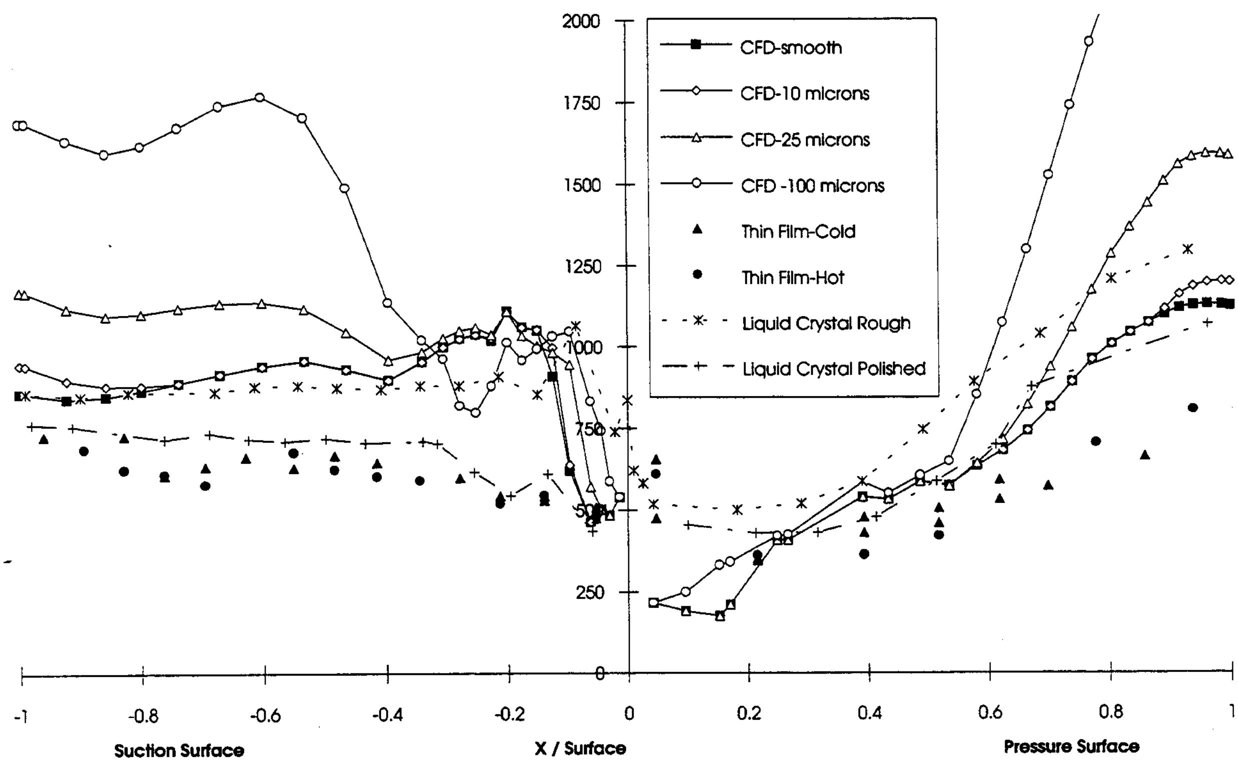

Figure 14 : Predicted and experimental measured heat transfer coefficient (W/m^{2}K)

Jones, T. V., 1991, *Definition of Heat Transfer Coefficient in the Turbine Situation,* IMechE Ç423/046.

Jones, T. V., 1988, *Gas Turbine Studies at Oxford 1969–1987,* ASME 88-GT-112.

Kays, W. M. and Crawford, M. E., 1993, *Convective Heat and Mass Transfer,* McGraw Hill.

Martinez-Botas, R. F., Lock, G. D., and Jones, T. V., 1994, *Heat Transfer Measurements in an Annular Cascade of Transonic Gas Turbine Blades Using the Transient Liquid Crystal Technique,* ASME 94-GT-172.

Martinez-Botas, R. F., Main, A. J., Lock, G. D., and Jones, T. V., 1993, *A Cold Heat Transfer Tunnel For Gas Turbine Research on an Annular Cascade,* ASME 93-GT-248.

Oldfield, M. L. G., Kiock, R., Holmes, A. T., and Graham, C. G., 1981, *Boundary Layer Studies on Highly Loaded Cascades using Heated Thin Films and Traversing Probe,* ASME J. of Engineering for Power, **(103)**, pp 237–246.

Oldfield, M. L. G., Jones, T. V. and Schultz, D. L., 1978, *On-Line Computer for Transient Turbine Cascade Instrumentation,* IEEE Transactions on Aerospace and Electronic Systems, AES-14, 5.

Prosser, T. J., 1994, *Heat Transfer and Loss Measurement in a Single-Stage Turbine with Film Cooling,* First Year Report, Oxford University.

Schultz, D. L., and Jones, T. V., 1973, *Heat Transfer Measurements in Short-Duration Hypersonic Facilities,* AGARD AG-165.

Turner, A. B., Tarada, F. H. A., and Bailey, F. J., 1985, *Effects of Surface Roughness on Heat Transfer to Gas Turbine Blades,* AGARD-CP-390.

Whitaker, S., 1977, *Fundamental Principles of Heat Transfer,* Pergamon Press.